Bollettino di Geofisica Teorica ed Applicata Vol. 52, n. 2, pp. x-xx; June 2011
DOI 10.4430/bgta0009

# Testing the stability of moment tensor solutions for small earthquakes in the Calabro-Peloritan Arc region (southern Italy)

S. D'Amico[1,6], B. Orecchio[2,3], D. Presti[3,4], A. Gervasi[2,5], L. Zhu[1], I. Guerra[2], G. Neri[3,5] and R.B. Herrmann[1]

[1] *Department of Earth and Atmospheric Sciences, University of St. Louis, MO, USA*
[2] *Dipartimento di Fisica, Università della Calabria, Arcavacata di Rende (CS), Italy*
[3] *Dipartimento di Scienze della Terra, Università di Messina, Italy*
[4] *Dipartimento di Scienze Geologiche, Università Roma Tre, Roma, Italy*
[5] *Istituto Nazionale di Geofisica e Vulcanologia, Roma, Italy*
[6] *Now at the Physics Department, University of Malta, Msida, Malta*

(Received: May 14, 2010; accepted: October 8, 2010)

***ABSTRACT*** The aim of this study is to test the stability of moment tensor solutions for crustal earthquakes in the Calabro-Peloritan area (southern Italy). We used waveforms recorded by the Italian National Seismic Network managed by the Istituto Nazionale di Geofisica e Vulcanologia and the CAT-SCAN (Calabria Apennine Tyrrhenian - Subduction Collision Accretion Network) project. We computed the moment tensor solutions using the Cut And Paste (CAP) method. The technique allows the determination of the source depth, moment magnitude and focal mechanisms using a grid search technique. For the earthquakes investigated, we tried different station distributions and different velocity models. Results were also checked by computing the moment tensor solutions using the SLUMT grid-search method. Both methods (CAP and SLUMT) allow time shifts between synthetic and observed data in order to reduce the dependence of the solution on the assumed velocity model and on earthquake location errors. Comparisons have been made with the available published solutions. The final focal mechanisms were robustly determined. We show that the application of the CAP and SLUMT methods can provide good-quality solutions in a magnitude range not properly represented in the Italian national earthquake catalogues, and where the solutions estimated from P-onset polarities are often poorly constrained.

**Key words:** moment tensor, focal mechanism, earthquake, southern Italy.

## 1. Introduction

In the last two decades, the use of waveforms recorded at local-to-regional distances has increased considerably. Waveform modeling has been used to estimate faulting parameters of small-to-moderate sized earthquakes (Mancilla *et al.*, 2002; Tan *et al.*, 2006; Zhu *et al.*, 2006; D'Amico *et al.*, 2008, 2010). It also has implications for seismic verification efforts and provides useful information for understanding the tectonic features of many regions where only small events are available to provide information on regional deformation.

 

The Calabro-Peloritan region (Fig. 1) is one of the areas with high seismic hazard (http://zonesismiche.mi.ingv.it; "Mappa di pericolosità sismica del territorio nazionale"). Based on the historical earthquake records the area has suffered intensity X or higher several times in the past centuries [for example in 1638, 1659, 1783, 1870, 1905, 1908, see Boschi *et al.* (2000) and CPTI Working Group (2004)]. In the last thirty years, crustal seismicity has been recorded in a low-to-moderate activity with just a few events having magnitude above 5 ["Catalogo della Sismicità Italiana" (CSI Working Group, 2001), "Bollettino Sismico Italiano" at http://bollettinosismico.rm.ingv.it/, ISIDE at http://iside.rm.ingv.it, and the catalogue of the regional seismic network of the University of Calabria]. The study area is also characterized by an intermediate and deep seismicity clustered and aligned along a narrow (less than 200 km) and steep (about 70°) Wadati-Benioff zone striking NE-SW and dipping towards the NW down to 500 km of depth (Piromallo and Morelli, 2003; Neri *et al.*, 2009). In the last thirty years, about a dozen, sub-crustal earthquakes with magnitude greater than 5 occurred in the study area.

Modeling regional seismograms for constraining moment tensors is widely accepted and largely documented by extensive literature. Modeling regional waveforms also provides a good constraint in accurately determining source mechanism and depth. Langston (1981) showed that it is possible to use the relative amplitude of P, SH, and SV waveforms to discriminate among fault types. Many attempts to model regional seismograms have been made in the last decades by using the body (Fan and Wallace, 1991; Dreger and Helmberger, 1993) and surface waves at different periods (Ritsema and Lay, 1993; Romanowicz *et al.*, 1993; Thio and Kanamori, 1995; Herrmann, 2008). However, the use of only surface waves requires a good azimuthal coverage around the source, which makes the application less effective in cases where only a few stations are available. The Cut and Paste (CAP) method (Zhu and Helmberger, 1996; Tan *et al.*, 2006) can be considered as a step forwards. In fact, by using this method, it is possible to separate the entire records into body waves (usually focusing on the P-waves) and surface waves and model them by allowing different time shifts. In doing so, this method desensitizes the timing between the principal crustal arrivals, so accurate source estimates can be achieved using Green's functions computed at nearby distances and with an approximate velocity model.

The final goal of this paper is to test the possibility of estimating faulting parameters of low magnitude events in the Calabro-Peloritan Arc region. We test the applicability of the CAP (Zhu and Helmberger, 1996; Tan *et al.*, 2006) and SLUMT (Herrmann, 2008) methods in order to implement the procedure for a successive compilation of a moment tensor catalogue for the area with an as low as possible magnitude threshold. This is important to improve the knowledge of the regional stress field and to understand the tectonic features of the area. Finally, for several earthquakes, we compare our solutions to those available in the RCMT [Regional Centroid Moment Tensor (Pondrelli *et al.*, 2006) at http://www.bo.ingv.it/RCMT/) and TDMT (Time Domain Moment Tensor (Scognamiglio *et al.*, 2009) at http://earthquake.rm.ingv.it/tdmt.php] catalogues, and computed by Li *et al.* (2007). It is important to remark that, for this region, just a small number of moment tensor solutions have been reported. Our results provide a key element, still partial, but useful, to constrain the regional tectonic processes in the Calabro-Peloritan Arc especially considering that the solutions estimated from P-onset polarities are often

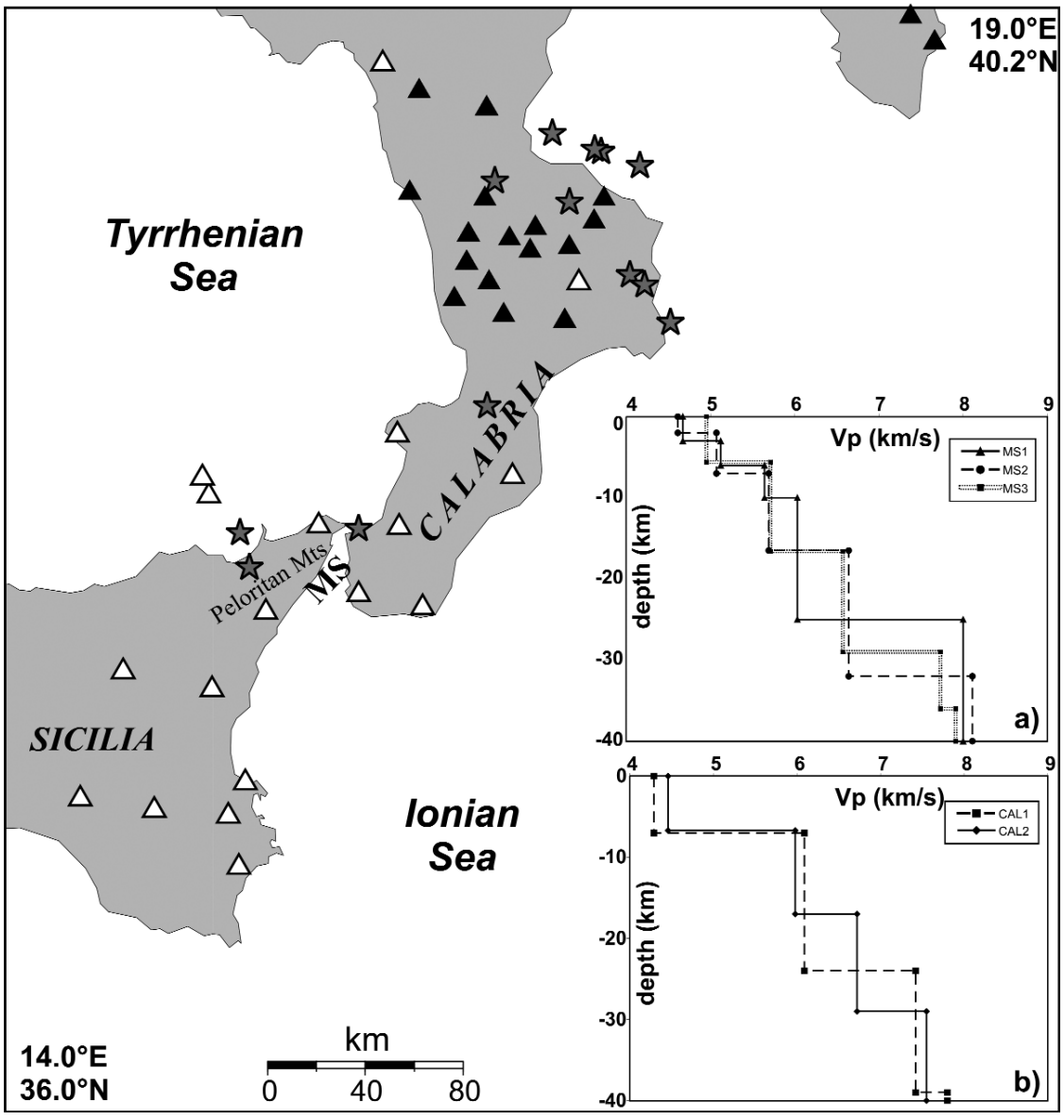


Fig. 1 - The map shows the investigated region (MS indicates Messina Straits). Triangles indicate location of the broadband stations (white and black triangles represent the INGV and CAT-SCAN stations respectively); gray stars indicate earthquakes investigated in this study. The velocity models used to compute Green's functions for the Messina Straits area (MS, plot a) and the Calabro region (CAL, plot b) are reported in the insets.

poorly constrained in this magnitude range.

## 2. Green's functions evaluation

Green's functions were computed using a 1-D velocity model with the frequency-wave

number method described by Zhu and Rivera (2002) and stored in a separate library in order to reduce the computational time. They represent the basic functions for all the double-couple mechanisms. To take into proper account the lithospheric heterogeneities, we used the most detailed 3-D velocity models available for the study region (Barberi *et al.*, 2004; Neri *et al.*, 2011) to derive a specific 1-D velocity model for each target area. To compute such 1-D model, we define sets of synthetic events and stations located at sea-level on regular two-dimensional grids covering the respective target area for the Messina Straits and Calabria region (MS and CAL) separately. For each pair of synthetic event-stations, we computed the theoretical travel times using the 3-D velocity models cited above and we used these data to build the relative plot of travel times versus epicentral distances. The data envelope may be fitted by a few piecewice continuous linear segments. Following the theory of travel-times in layered media (see e.g., Lay and Wallace, 1995), we estimated both velocity and thickness of the layers needed to build the 1-D velocity model. With this approach, we may reconstruct a 1-D velocity model "equivalent" to the 3-D one for a specific set of synthetic ray-paths. The chosen configuration of events and stations allows us to sample the investigated region with a high density of seismic paths also showing a very robust ray crossing and therefore the "equivalent" 1-D velocity model may be considered a good approximation of the local 3-D structure. In order to test the stability of the CAP solutions with respect to velocity structure variations, we estimated several different models for each sector (i.e., MS and CAL) by changing (i) the stations/earthquakes distribution (2D grids, hypocenter locations of the real earthquakes with the relative network geometries) or (ii) the starting 3-D velocity model (Barberi *et al.*, 2004; Neri *et al.*, 2011) or (iii) the branches chosen for the best fits. For conciseness, we report only the results for five models (MS1, MS2, and MS3 of the Messina Straits and CAL1 and CAL2 of the Calabria region) chosen as representative of the local lithospheric heterogeneities. The insets of Fig. 1 show the crustal velocity models used for computing Green's functions. Green's functions have been computed for a distance range from 5 to 500 km with a spacing of 5 km and a focal depth range from 1 to 50 km due to the crustal nature of the investigated earthquakes (H<40 km).

## 3. "Cut and paste" method

The synthetic seismogram for a double-couple mechanism, *s(t)*, is defined as:

$$s(t) = M_0 \sum_{i=1}^{3} A_i(\phi - \theta, \delta, \lambda) \cdot G_i(t) \qquad (1)$$

where $M_0$ is the scalar moment, $A_i$ represents the radiation coefficient and $\phi, \theta, \delta$, and $\lambda$ represent the station azimuth, strike, dip, and rake of the source. $G_i(t)$ are Green's functions with $i$=1, 2, 3 corresponding to the three fundamental faults (i.e., vertical strike-slip, vertical dip-slip, and 45° dip-slip). If $u(t)$ is defined to be the observed data and if the synthetics reproduce the real data perfectly:

$$u(t) = s(t). \qquad (2)$$

Since the above equation leads to a non-linear problem, it is convenient to solve the problem with a grid search method. In order to measure the misfit error between observed and synthetic data, we define an object function and search through the parameter space to find the global minimum of the object function. The misfit error is defined as the norm of the difference between observed and synthetic data multiplied by another term that takes into account the distance range scaling. Mathematically it can be defined as:

$$e = \left\| \left( \frac{r}{r_0} \right)^p \right\| \cdot \left\| u(t) - s(t) \right\| \tag{3}$$

where $p$ is a scaling factor to give the record at distance $r$ the same weight as that at reference distance $r_0$. To weight the Pnl (defined as the first arrival from seismic source in the crust corresponding to waves reflected and multireflected from the top of the sharpest discontinuity) and the surface wave we assume a spherical geometrical spreading for body waves ($p$=1) and a cylindrical geometrical spreading for surface waves ($p$=0.5). The scaling factor avoids the problem caused by using the true-amplitude waveforms which make the closest stations dominate the inversion (Zhu and Helmberger, 1996). The radiation pattern is taken out so the decay with distance is related only to the amplitude decay due to the geometrical spreading. In particular, we use the chi-square, $\chi^2$, as our object function

$$\chi^2 = \frac{e_{Pnl}}{\sigma_{Pnl}^2} + \frac{e_{surf}}{\sigma_{surf}^2} \tag{4}$$

where the waveform misfit errors are defined as the following:

$$e_{Pnl} = \left\| u^{Pnl}(t) - s^{Pnl}\left(t - \Delta T^{Pnl}\right) \right\| \tag{5}$$

$$e_{surf} = \left\| u^{Rayleigh}(t) - s^{Rayleigh}\left(t - \Delta T^{Rayleigh}\right) \right\| + \left\| u^{Love}(t) - s^{Love}\left(t - \Delta T^{Love}\right) \right\| \tag{6}$$

here the symbol $\| \ \|$ denotes the L2 norm. $\Delta T$ represents the time-shift required to align synthetics with data. In Eq. (4), the terms at the denominator are the variance of waveform residuals of the Pnl and surface waves. They measure how well the velocity model can explain the observed data. We simply search through the whole parameter space of all the unknowns (depth/strike/dip/rake) and determine the best solution of the source parameters. For additional details we refer to Zhu and Helmberger (1996) and Tan *et al.* (2006).

## 4. Data set

We started by compiling a list of all earthquakes in the study area from the seismic catalogue

Table 1 - Source parameters of the earthquakes used in this study. Date, origin time and epicentral coordinates are taken from ISIDE-INGV seismic catalogue (http://iside.rm.ingv.it). The CAP method has been used for computation of the focal depth (H), the fault parameters (strike, dip and rake), and the moment magnitude $M_w$.

| Event ID | Date | O.T. | Lat N (°) | Lon E (°) | H (km) | Strike (°) | Dip (°) | Rake (°) | Mw |
|---|---|---|---|---|---|---|---|---|---|
| 20050131 | 31/01/2005 | 10.44.50 | 39.6630 | 16.8640 | 30 | 23 | 79 | -41 | 4.1 |
| 20050423 | 23/04/2005 | 19.11.43 | 39.4740 | 16.7110 | 23 | 128 | 58 | 14 | 4.1 |
| 20051203 | 03/12/2005 | 8.33.03 | 39.2035 | 17.0021 | 15 | 290 | 64 | -18 | 3.8 |
| 20050907 | 09/07/2005 | 12.40.33 | 38.7130 | 16.3170 | 16 | 80 | 90 | -42 | 3.6 |
| 20051118 | 18/11/2005 | 18.35.25 | 39.1665 | 17.0731 | 23 | 120 | 34 | 3 | 3.6 |
| 20060227 | 27/02/2006 | 4.34.01 | 38.1017 | 15.1730 | 10 | 62 | 50 | -71 | 4.1 |
| 20060417 | 17/04/2006 | 2.44.06 | 39.6096 | 17.0504 | 28 | 114 | 74 | -3 | 4.4 |
| 20060622 | 22/06/2007 | 19.34.58 | 39.7307 | 16.6310 | 30 | 151 | 42 | 81 | 4.6 |
| 20070426 | 26/04/2007 | 0.49.36 | 39.5546 | 16.3542 | 13 | 231 | 22 | -23 | 3.9 |
| 20070525 | 25/05/2007 | 9.39.45 | 39.6715 | 16.8325 | 25 | 91 | 29 | -48 | 4.2 |
| 20070801 | 01/08/2007 | 0.07.54 | 39.0247 | 17.1971 | 40 | 80 | 67 | -45 | 4.1 |
| 20070818 | 18/08/2007 | 14.04.07 | 38.2316 | 15.1291 | 9 | 44 | 50 | -23 | 3.9 |
| 20080413 | 13/04/2008 | 13.06.57 | 38.2488 | 15.6992 | 14 | 6 | 51 | -30 | 2.8 |

of the Istituto Nazionale di Geofisica e Vulcanologia (INGV) (http://iside.rm.ingv.it) for the time period from October 2004 to May 2008 with focal depths of less than 40 km. The data set was restricted to the earthquakes recorded at a minimum of 4, three-component seismic stations located within about 200 km from the epicenter. We used seismograms recorded by the Italian National Seismic Network, managed by the INGV, and by the Calabria Apennine Tyrrhenian - Subduction Collision Accretion Network (CAT-SCAN, http://www.ldeo.columbia.edu/res/pi/catscan). During the CAT-SCAN project, researchers from the Lamont-Doherty Earth Observatory, INGV and University of Calabria, deployed 40 portable digital broadband seismographs throughout southern Italy. The stations were equipped with Reftek130 or Reftek72A07 data loggers and several three-component, sensor types (i.e., CMG40T, CMG3T, L-22, STS2, TRILLIUM40, CMG3ESP). Fig. 1 shows the location of seismic stations and epicenters used in this study; the earthquakes used in our test are listed in Table 1. Each waveform was examined to eliminate recordings with spurious transients or low signal-to-noise ratios and corrected for the instrument response to yield ground velocity. Finally, the picking of P-arrivals were reviewed and the horizontal recordings were rotated to radial and transverse components.

## 5. Results and discussion

The main advantage of the CAP method is that it has little sensitivity to the velocity model and lateral crustal variation. The technique "cuts" broadband waveforms into the Pnl and surface wave segments that can be inverted independently. The surface wave segments are larger in amplitude than the Pnl waves and can be affected by the shallow crustal heterogeneities. The Pnl waves have a lower signal-to-noise ratio and are mainly controlled by the average crustal velocity

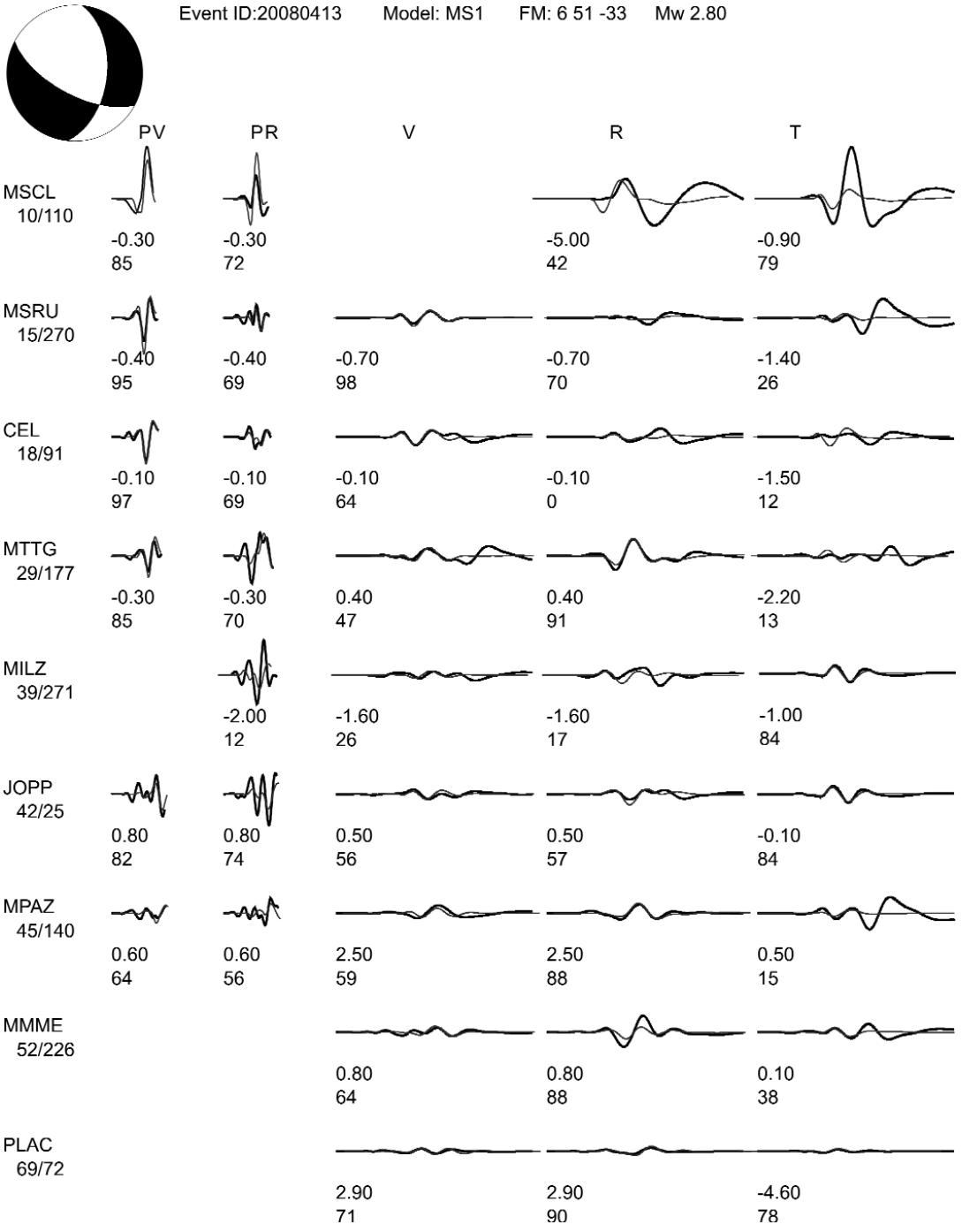


Fig. 2 - Example of waveform fit (Event ID 20080413). Black and gray traces indicate the observed and synthetic data, respectively. The two left columns show the waveform fits for the Pnl waves, while the next three show the waveform fits for the vertical, radial and tangential components of the surface wave segments, respectively. The numbers below each trace segment are the time shifts (in seconds) and the cross-correlation coefficients. The numbers below the name of the seismic station are the distance source-station and azimuth, respectively.

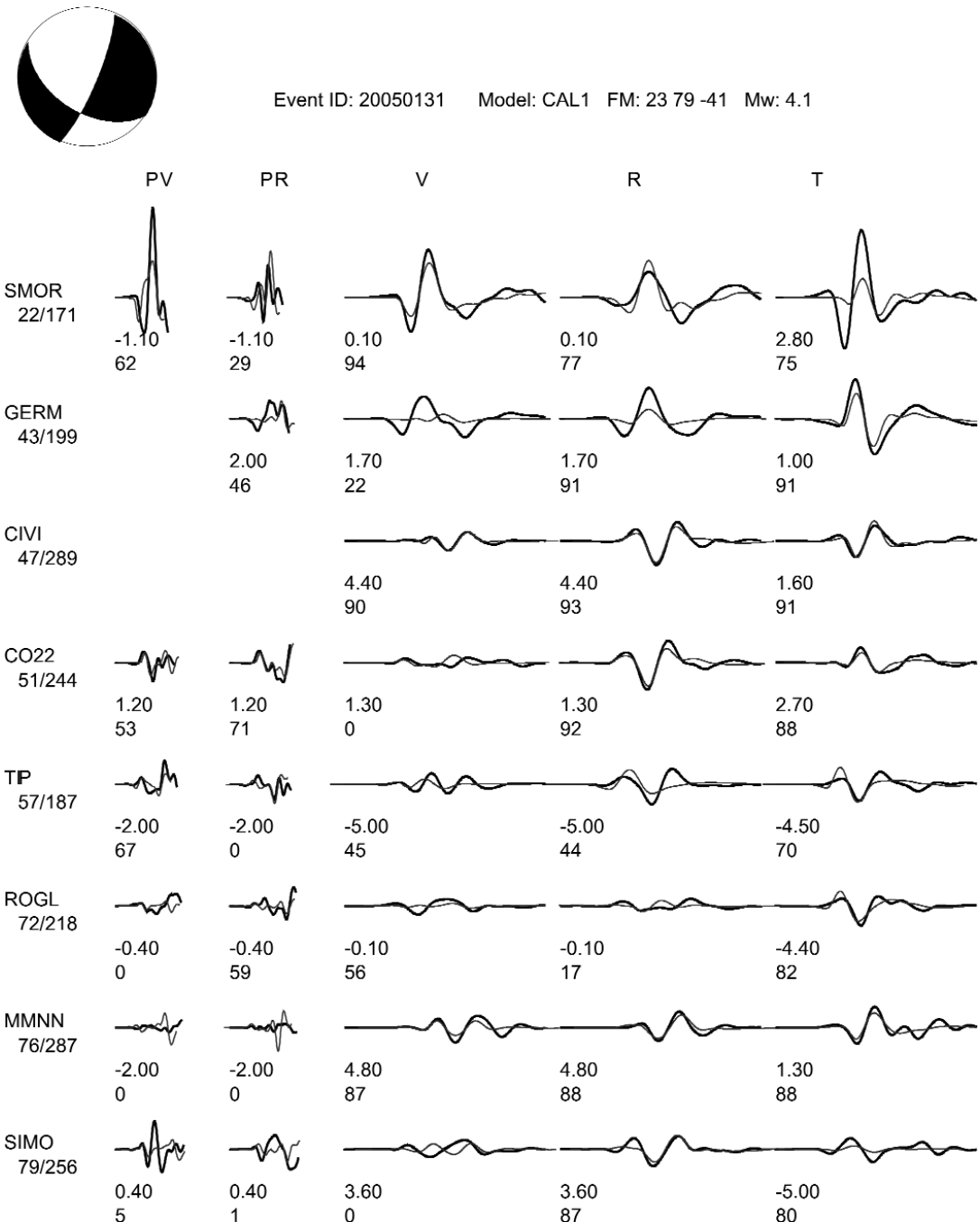


Fig. 3 - Example of waveform fit (Event ID 20050131). See caption of Fig. 2 for details.

structure. For this reason, we weighted the body wave segments more by multiplying their amplitude by a factor of 2. Using the whole seismogram implies that the inversions are mainly controlled by surface waves. We preferred to use ground velocity rather than ground

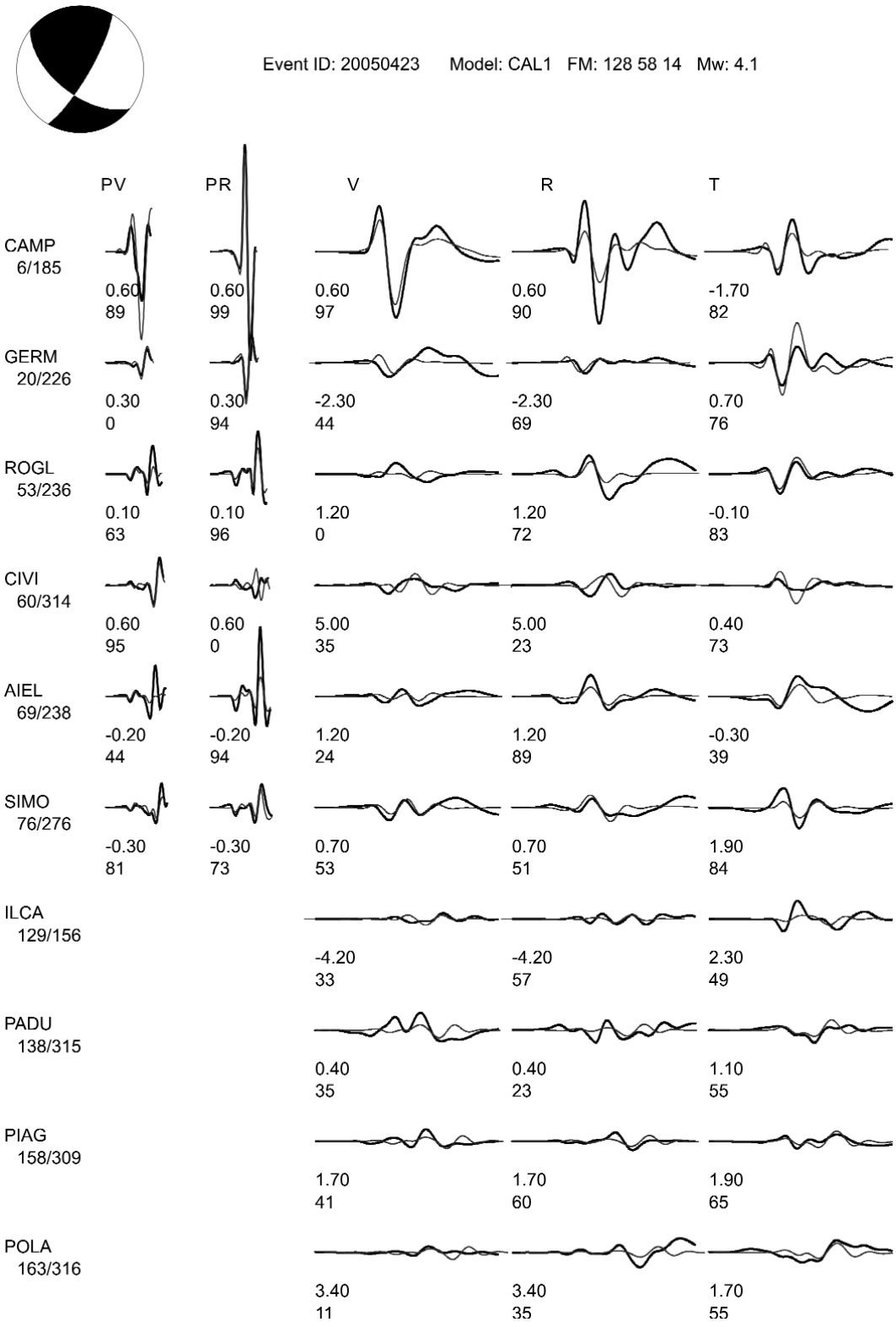


Fig. 4 - Example of waveform fit (Event ID 20050423). See caption of Fig. 2 for details.

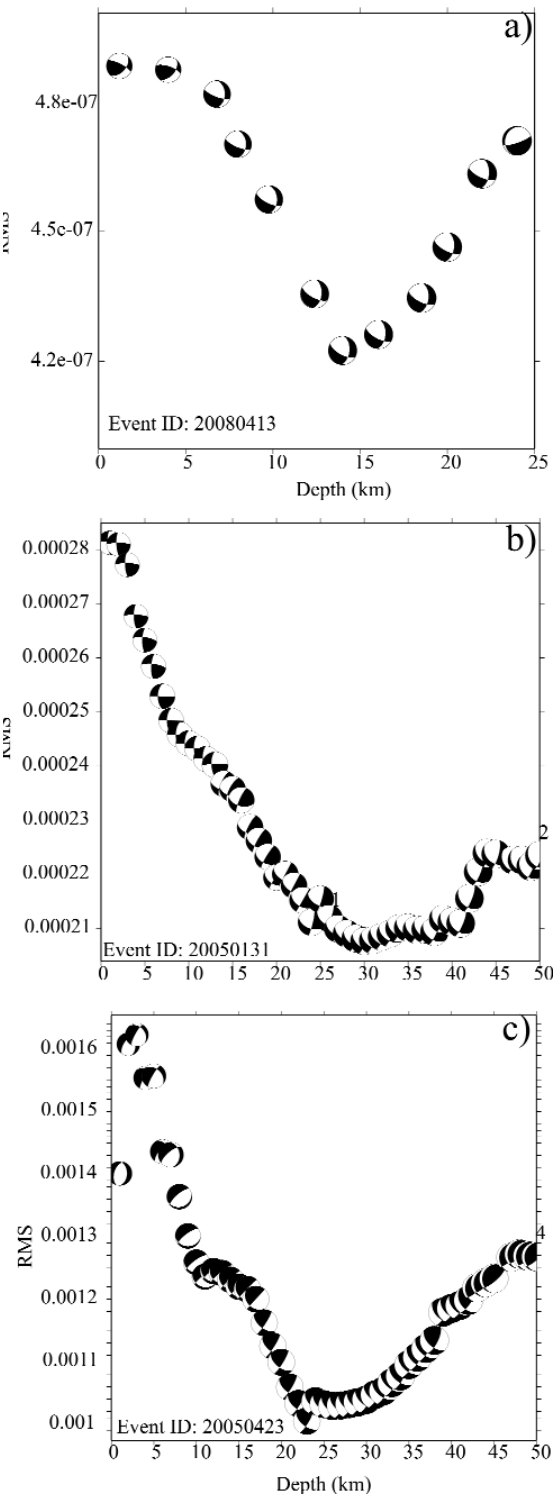


Fig. 5 - Misfit error as a function of depth for the Event ID 20080413 (a), 20050131 (b), and 20050423 (c). The solution does not change around the minimum indicating the stability of the final solution.

displacement mainly because we used weak-motion data. Another reason is that for the earthquakes having magnitude less than 4 there is high signal-to-noise ratio only at the higher frequencies. Furthermore, working with ground velocity rather than displacement reduces the influence of a low frequency site or instrument noise on the deconvolution. In addition, the moment tensor inversion, at regional distances, is possible if the bandpass filtered waveforms are simple in appearance and can be modeled with a 1-D Earth model. The choice of frequency band depends on the magnitude of the event. The typical frequency bands we used in the present study are from 0.05 Hz to 0.3 Hz for the Pnl and from 0.02 Hz to 0.1 Hz for surface waves. However, to determine the moment tensor solution for smaller earthquakes, it is necessary to consider higher frequencies.

Figs. 2, 3, and 4 report examples of the waveform fits produced by the CAP inversion for three different events. Black and gray traces indicate the observed and synthetic data, respectively. There are several reasons for larger time shifts compared to travel time residuals from earthquake location. First, Green's functions were computed every 5 km in epicentral distance, so that the synthetics were often not located at the same distance as the observation. Second, the time shifts were determined by waveform cross-correlation instead of the first P onset as in travel time. Given the complicated crustal structure of the study area, particularly in the shallow part, it is not surprising to have several seconds of time delays for surface waves and bad waveform fits at a few stations. Furthermore, the amplitudes could not match perfectly in some cases since we are not taking into account the possible effects to the local geology at the recording site. The moment

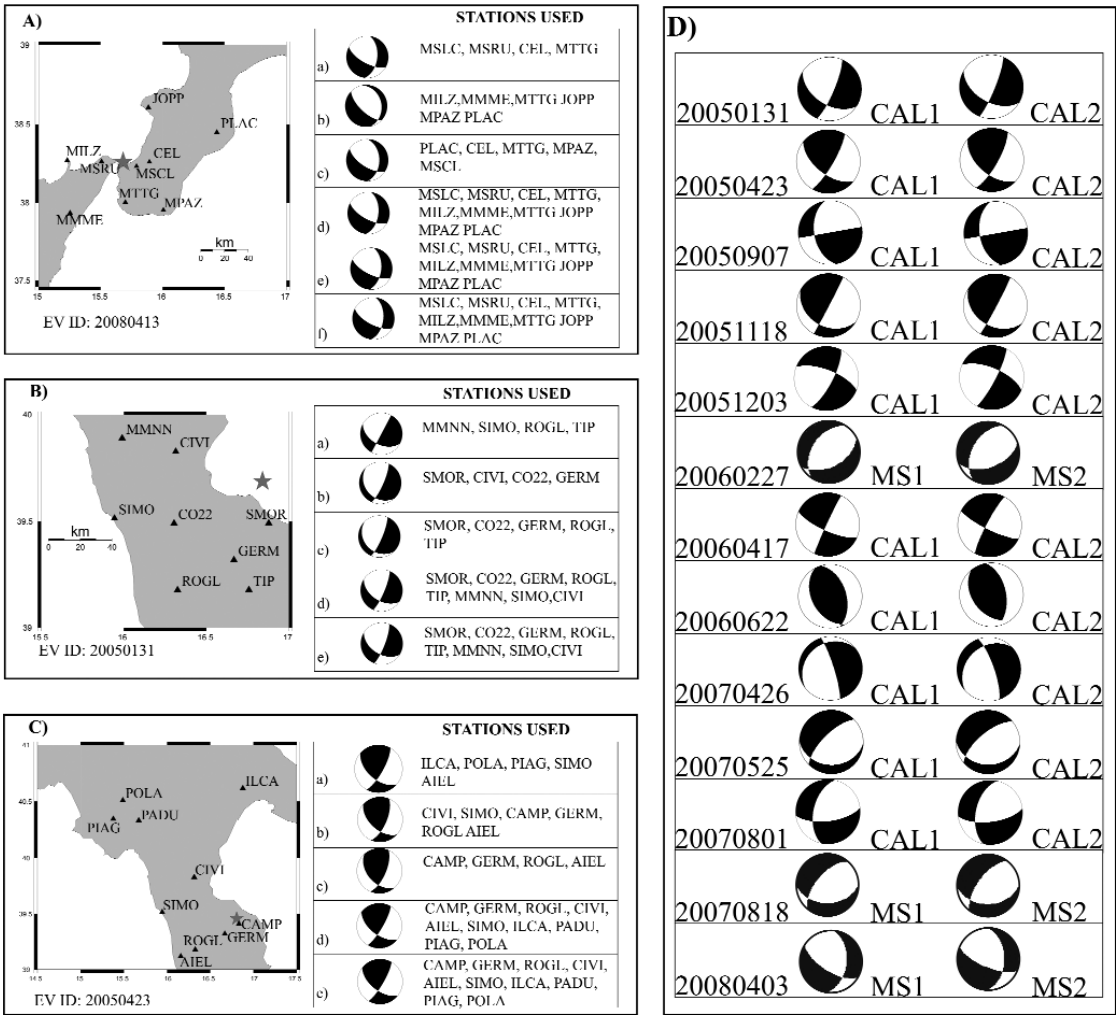


Fig. 6 - Example of tests performed in order to verify the stability of the final focal mechanism. Panel A, B and C show several tests for Event ID 20080413, 20050131 and 20050423. In each case, the tests a, b, and c show the focal mechanism obtained by using different stations. Test d reports the solution forcing the epicenter to lie 5 km south with respect of the true location. Tests e and f, report the mechanisms estimated using different velocity models (Fig. 1). In particular, we used the velocity models MS2 and MS3 to obtain the focal mechanisms of the tests e and f for Event ID 20080413. Model CAL2 was used to compute the solution (test e) reported in panel B for Event ID 20050131 and in panel C for Event ID 20050423 (just for this event we used some stations not reported in Fig. 1). Panel D shows the comparison of the focal mechanisms of the earthquakes listed in Table 1 obtained by applying the CAP method and using the different velocity models for the earthquakes in the Calabro and Peloritan region, respectively. The velocity model used to obtain the focal mechanism is reported on the right of each fault plane solution.

tensor solutions and focal depths, however, are robust when we had good waveform fits at the majority of stations. Fig. 5 shows the misfit error as a function of depth for the events in Figs. 2, 3 and 4. It is possible to notice that the solutions do not change around the minimum, indicating the stability of the final solution.

A good focal mechanism estimation can be obtained using a few stations or even only two

Table 2 - Source parameters (strike, dip and rake) of focal mechanisms reported in Fig. 7.

| Event ID | CAP | TDMT | RCMT | Li *et al.* (2007) | SLUMT |
|---|---|---|---|---|---|
| | strike/dip/rake (°) | strike/dip/rake (°) | strike/dip/rake (°) | strike/dip/rake (°) | strike/dip/rake (°) |
| 20050131 | 23/79/-41 | N.A. | N.A. | 28/78/-180 | 35/70/-25 |
| 20050423 | 128/58/14 | N.A. | N.A. | 281/59/125 | 290/80/-15 |
| 20050907 | 80/90/-42 | N.A. | N.A. | 164/78/-180 | N.A. |
| 20051118 | 120/34/3 | N.A. | N.A. | 121/33/-12 | N.A. |
| 20060227 | 62/50/-71 | N.A. | 218/29/-62 | N.A. | 65/50/-85 |
| 20060417 | 114/74/ -3 | 225/81/-144 | 318/72/-15 | 239/84/-159 | 130/65/15 |
| 20060622 | 151/42/ 81 | 348/57/101 | 157/33/88 | 110/70/16 | 150/42/55 |
| 20070426 | 231/22/-23 | 298/54/-126 | N.A. | N.A. | 225/40/-35 |
| 20070525 | 91/29/-48 | 230/84/-101 | N.A. | N.A. | 160/25/-10 |
| 20070801 | 80/67/-45 | 55/74/56 | N.A. | N.A. | 85/75/-50 |
| 20070818 | 44/50/-23 | 344/79/168 | N.A. | N.A. | 44/50/-23 |

stations with an azimuthal gap of about 180 degrees (Dreger and Helmberger, 1993; Zhu and Helmberger, 1997; D'Amico *et al.*, 2010). Fig. 6 presents, for the events in Figs. 2, 3, and 4, the tests we have done to investigate the stability of the final focal mechanism. We varied, for example, the number of stations used, the azimuthal coverage or the use of different velocity models, with the final mechanism being robust. In fact, we found that just a few stations provide enough information to properly constrain the focal mechanism of the earthquake. Furthermore, we note that azimuthal gaps as large as 180° in station distributions, do not significantly change the solution. Panel D of Fig. 6 shows the comparison of the focal mechanisms of the earthquakes listed in Table 1 obtained by applying the CAP method and using different velocity models for the studied earthquakes. The high stability of CAP solutions when the model changes is evident.

For the investigated events, we also applied the SLUMT waveform inversion technique (Herrmann, 2008) to get the moment tensor solution as an additional check. The approach models the entire ground velocity waveform and uses a different technique to compute Green's functions (Herrmann, 2002). Data processing for the waveform inversion consisted of a deconvolution to ground velocity in units of m/s and a quality control check on the resulting waveforms. Both the observed ground velocities and Green's function were filtered between 0.02 and 0.10 Hz using three-pole Butterworth highpass and lowpass filters, respectively. The method performs a grid search over the focal mechanism parameters of strike, dip and rake angles and source depth (Herrmann, 2008; Herrmann *et al.*, 2008). With the SLUMT method, we model the entire wavetrain and for this reason the inversion is mainly controlled by the surface wave amplitudes.

For a few events in the area there are moment tensor solutions by Li *et al.* (2007), and the solutions published by INGV in the RCMT and TDMT catalogues. Fig. 7 shows a comparison of the source mechanisms obtained among the different approaches. The RCMT solutions are usually released for intermediate-sized earthquakes ($4.5<M<5.5$), and are rare for smaller earthquakes because, in this case, the solutions tend to be less constrained (http://www.bo.ingv.it/RCMT/). This is the reason

| Event ID | CAP | TDMT | RCMT | Li et al. (2007) | SLUMT |
|---|---|---|---|---|---|
| 20050131 |  | N.A. | N.A. |  91.8 |  19.7 |
| 20050423 |  | N.A. | N.A. |  103.5 |  45.7 |
| 20050907 |  | N.A. | N.A. |  30.6 | N.A. |
| 20051118 |  | N.A. | N.A. |  15.0 | N.A. |
| 20060227 |  | N.A. |  48.6 | N.A. |  15.7 |
| 20060417 |  | A  27.9 |  45.1 |  11.3 |  21.6 |
| 20060622 |  | A  9.4 |  10.0 |  58.7 |  25.3 |
| 20070426 |  | C  55.3 | N.A. | N.A. |  19.8 |
| 20070525 |  | A  17.8 | N.A. | N.A. |  38.9 |
| 20070801 |  | B  103.4 | N.A. | N.A. |  11.3 |
| 20070818 |  | C  44.1 | N.A. | N.A. |  0.0 |

Fig. 7 - Focal mechanisms comparison. Kagan (1991) angles are reported on the right of each solution compared to the respective CAP solution. Quality of TDMT solutions is also reported (see text for details).

why just three focal mechanisms are available in the area for the time period considered in this study. The TDMT solutions are obtained by applying the procedure proposed by Dreger (2003). The TDMT solutions are usually obtained using a small number of stations, but with an as good as possible azimuthal coverage. However, if the azimuthal coverage is not optimal, the final solution may not be well constrained, consequently the solution is labeled as "Quality C" or "Quality D". The given quality of the solution is also dependent on the variance reduction. A solution is labeled as "Quality A" if the moment tensor has variance reduction greater that 60% obtained by using 4-8 stations (Scognamiglio *et al.*, 2009). The focal mechanisms reported by Li

*et al.* (2007) were obtained by applying the CAP method, but using a different velocity model to compute Green's functions and by adopting different source-receiver geometries because of the use of seismograms recorded only from the INGV seismic network. Table 2 reports the strike, dip and rake angles for the focal mechanisms shown in Fig. 7.

The agreement between CAP solutions and the others reported in Fig. 7 have been numerically checked by applying the method by Kagan (1991). The Kagan angle measures the rotation that should be applied to one earthquake source double-couple to make it coincident with another one. It may vary from 0° (indicating perfect agreement between the two solutions) to 120° (total disagreement), thus values well below 60° indicate a good correspondence while above 60° a mismatch (Pondrelli *et al.*, 2006). The results of the comparison are shown in Fig. 7. The agreement is very good between both CAP vs. SLUMT and CAP vs. RCMT solutions, 83% between CAP and TDMT solutions [note that the Kagan (1991) angles are smaller for "A" quality TDMT solutions] and only 66% between CAP and Li *et al.* (2007) solutions. In general, the differences among the solutions in Fig. 7 can be due to a combination of several factors: (I) the adoption of different velocity models to compute Green's functions, (II) the use of different stations and different azimuthal coverage; (III) the use of diverse frequency bands; (IV) the use of ground displacement versus ground velocity. It is important to remark that the CAP method uses higher frequency P-waves featuring a larger resolving power than lower frequency methods. Furthermore, the use of many stations increases the reliability of the focal mechanism because of the large number of waveforms fitted simultaneously. The stability of the tests discussed above, the quality of waveform fit (see, e.g., Fig. 5) together with the good agreement between CAP and other solutions, in particular with those coming from the SLUMT and RCMT methods, lead us to believe that the final focal mechanisms obtained in this study are robustly determined.

## 6. Conclusion

Earthquake source parameters play a key role in several seismological researches. Moment tensor solutions provide the source focal mechanisms (strike/dip/rake of possible fault plane), depth and moment magnitude allowing us, for example, to constrain regional seismo-tectonic deformations and the stress field. Focal mechanisms estimated with the traditional method of P-wave first motion are usually affected by inherent uncertainties, and they might be unstable because of insufficient azimuthal coverage and are not easily determined for low magnitude events. In addition, the RCMT and TDMT catalogue report only a few moment tensor solutions in the investigated region. Thus, the knowledge derived from earthquake focal mechanisms in this area can be considered limited.

In this study, we provide moment tensor solutions for several events of small magnitude in the Calabro-Peloritan Arc. We used waveforms recorded by the Italian National Seismic Network and managed by the INGV and the CAT-SCAN project. We computed the moment tensor solutions using the CAP and SLUMT methods and we tested the stability of the final solutions by investigating the effects of using different stations or velocity models. Comparisons have been made also with the published solutions available. We conclude that the final focal mechanisms were robustly determined. Furthermore, we show that the application of the CAP and SLUMT methods can provide good-quality solutions in the area in a magnitude range not properly

represented in the Italian national catalogues and where the solutions estimated from P-onset polarities are often poorly constrained. In the near future, by applying the CAP and SLUMT methods, we expect to provide several more moment tensor solutions to improve the knowledge of the seismo-tectonic regime, the regional stress field features, and the seismic hazard in the Calabro-Peloritan Arc.

**Acknowledgements.** The authors thank the Calabria-Apennine-Tyrrhenian/Subduction-Accretion-Collision Network (CAT/SCAN) participants and the "Istituto Nazionale di Geofisica e Vulcanologia" for having provided high quality seismic data. Thanks are also due to the editor Dario Albarello, Simone Salimbeni and an anonymous reviewer for comments and suggestions. Some figures were created using the Generic Mapping Tools (GMT) by Wessel and Smith (1991).

## REFERENCES

Barberi G., Cosentino M.T., Gervasi A., Guerra I., Neri G. and Orecchio B.; 2004: *Crustal seismic tomography in the Calabrian Arc region, south Italy*. Phys. Earth Planet. Int., **147**, 297-314.

Boschi E., Guidoboni E., Ferrari G., Mariotti D., Valensise G. and Gasperini P. (eds); 2000: *Catalogue of Strong Italian Earthquakes from 461 B.C. to 1997*. Ann. Geofis., **43**, 609-868.

CPTI Working Group; 2004: *Catalogo Parametrico dei Terremoti Italiani*, *versione 2004 (CPTI04)*. Istituto Nazionale di Geofisica e Vulcanologia, Bologna, http://emidius.mi.ingv.it/CPTI/home.html (last access 2010 March 1).

CSI Working Group; 2001: *Catalogo della Sismicità Italiana*. Istituto Nazionale di Geofisica e Vulcanologia, http://csi.rm.ingv.it (last access 2010 March 1).

D'Amico S., Orecchio B., Presti D., Zhu L., Herrmann R.B. and Neri G.; 2008: *Moment tensor solutions in the area of the 1908 Messina earthquake: preliminary results*. Miscellanea INGV, **8**, 43-44.

D'Amico S., Orecchio B., Presti D., Zhu L., Herrmann R.B. and Neri G.; 2010: *Broadband waveform inversion of moderate earthquakes in the Messina Straits, Southern Italy.* Phys. Earth Planet. Int., **179**, 97-106, doi: 10.1016/j.pepi.2010.01.012.

Dreger D.S.; 2003: *TDMT_INV: Time domain seismic moment tensor inversion*. In: Lee W.H.K., Kanamori H., Jennings P.C. and Kisslinger C. (eds). International Handbook of Earthquake and Engineering Seismology, Vol. B, Academic Press, An Imprint of Elsevier Science, London, 1627 pp.

Dreger D.S. and Helmberger D.V.; 1993: *Determination of source parameters at regional distances with single station or sparse network data.* J. Geophys Res., **98**, 1162-1179.

Fan G. and Wallace T.; 1991: *The determination of source parameters for small earthquakes from a single, very broadband seismic station*. Geophys. Res. Lett., **18**, 1385- 1388.

Herrmann R.B.; 2002: *An overview of synthetic seismogram computation, computer programs in Seismology*. Saint Louis University, 183 pp.

Herrmann R.B.; 2008: *Toward automated focal mechanism and moment determination for the continental U.S. - an ANSS product.* Final Technical Report USGS Grant 05HQGR0047, 16 pp.

Herrmann R.B., Withers M. and Benz H.; 2008: *The April 18, 2008 Illinois earthquake: an ANSS monitoring success*. Seism. Res. Lett., **79**, 830-843.

Kagan Y.Y.; 1991: *3-D rotation of double-couple earthquake sources.* Geophys. J. Int., **106**, 709-716.

Langston C.A.; 1981: *Source inversion of seismic waveforms: the Koyna, India, earthquakes of 13 September 1967*. Bull. Seismol. Soc. Am., **71**, 1-24.

Lay T. and Wallace T.C.; 1995: *Modern global Seismology*. Academic Press, San Diego, 521 pp.

Li H., Michelini A., Zhu L., Bernardi F. and Spada M.; 2007: *Crustal velocity structure in Italy from analysis of regional seismic waveforms*. Bull. Seism. Soc. Am., **97**, 2024-2039, doi: 10.1785/0120070071.

Mancilla F., Ammon C.J., Herrmann R.B., and Morales J.; 2002: *Faulting parameters of the 1999 Mula earthquake, southern Spain.* Tectonophysics, **354**, 139-155.

Neri G., Marotta A.M., Orecchio B., Presti D., Totaro C., Barzaghi R. and Borghi A.; 2011: *How lithospheric subduction changes along the calabro arc in southern Italy: geophysical evidences*. Geophys. J. Int., submitted.

Neri G., Orecchio B., Totaro C., Falcone G. and Presti D.; 2009: *Subduction beneath southern Italy close the ending: results from seismic tomography*. Seim. Res. Lett., **80**, 63-70.

Piromallo C. and Morelli A.; 2003: *P wave tomography of the mantle under the Alpine-Mediterranean area*. J. Geophys. Res., **108**, B2, 2065, 23 pp., doi: 10.1029/2002JB001757.

Pondrelli S., Salimbeni S., Ekström G., Morelli A., Gasperini P. and Vannucci G.; 2006: *The Italian CMT dataset from 1977 to the present*. Phys. Earth Planet. Int., **159**, 286-303, doi: 10.1016/j.pepi.2006.07.008.

Ritsema J. and Lay T.; 1993: *Rapid source mechanism determination of large earthquakes in the western United States*. Geophys. Res. Lett., **20**, 1611-1614.

Romanowicz B., Dreger D., Pasyanos M. and Uhrhammer R.; 1993: *Monitoring of strain release in central and northern California*. Geophys. Res. Lett., **20**, 1643-1646.

Scognamiglio L., Tinti E. and Michelini A.; 2009: *Real-Time Determination of Seismic Moment Tensor for the Italian Region*. Bull. Seism. Soc. Am., **99,** 2223-2242.

Tan Y., Zhu L., Helmberger D. and Saikia C.; 2006: *Locating and modeling regional earthquakes with two stations*. J. Geophys. Res., **111**, B01306, 15pp.

Thio H.-K. and Kanamori H.; 1995: *Moment-tensor inversions for local earthquakes using surface waves recorded at TERRAscope*. Bull. Seismol. Soc. Am., **85**, 1021-1038.

Wessel P. and Smith W.H.F.; 1991: *Free software helps map and display data*. Eos Trans., AGU, **72**, 441.

Zhu L. and Helmberger D.; 1996: *Advancement in source estimation technique using broadband regional seismograms*. Bull. Seism. Soc. Am., **86**, 1634-1641.

Zhu L. and Helmberger D.; 1997: *Regional waveform calibration in the Pamir-Hindu Kush region.* J. Geophys. Res., **102**, 22799-22813.

Zhu L. and Rivera L.A.; 2002: *A note on the dynamic and static displacement from a point source in multi-layered media.* Geophys. J. Int., **148**, 619-627.

Zhu L., Akyol N., Mitchell B. and Sozbiliz H.; 2006: *Seismotectonics of western Turkey from high resolution earthquake relocations and moment tensor determinations*. Geophys. Res. Lett., **33**, L07316, 4 pp.

*Corresponding author:* Sebastiano D'Amico
Physics Department
University of Malta, Msida, Malta
Phone: +356 2340 3034; fax: +356 2133 2728; e-mail: sebdamico@gmail.com